Synergistic Effects on Escape of a Ligand from the Closed Tryptophan Synthase Bienzyme Complex†

Rodney M. Harris,‡ Huu Ngo,§ and Michael F. Dunn*,§

Department of Biochemistry, University of California, Riverside, California 92521, and The Scripps Research Institute, 10550 North Torrey Pines Road, La Jolla, California 92037-1000

Received August 24, 2005; Revised Manuscript Received October 15, 2005

ABSTRACT: Substrate channeling in the tryptophan synthase bienzyme complex is regulated by allosteric signals between the α- and β-active sites acting over a distance of 25 Å. At the α-site, indole is cleaved from 3-indole-D-glycerol 3′-phosphate (IGP) and is channeled to the β-site via a tunnel. Harris and Dunn [Harris, R. M., and Dunn, M. F. (2002) *Biochemistry 41*, 9982−9990] showed that when the novel amino acid, dihydroiso-L-tryptophan (DIT), reacts with the β-site, the α-aminoacrylate Schiff base, E(A-A), is formed and the enzyme releases indoline. The indoline produced exits the enzyme via the tunnel out the open α-site. When the α-site ligand (ASL) α-D,L-glycerol 3-phosphate (GP) binds and closes the α-site, indoline generated in the DIT reaction is trapped for a short period of time as the quinonoid intermediate in rapid equilibrium with bound indoline and the E(A-A) intermediate before leaking out of the closed enzyme. In this work, we use the DIT reaction and a new, high-affinity, ASL, *N*-(4-trifluoromethoxybenzenesulfonyl)-2-amino-1-ethyl phosphate (F9), to explore the mechanism of ligand leakage from the closed enzyme. It was found that F9 binding to the α-site is significantly more effective than GP in trapping indoline in the DIT reaction; however, leakage of indoline from the enzyme into solution still occurs. It was also found that a combination of benzimidazole (BZI) and GP provided even more effective trapping than F9. The new experiments with F9 and the combination of BZI and GP provide evidence that the coincident binding of GP and BZI at the α-site exhibits a strong synergistic effect that greatly slows the leakage of indoline in the DIT reaction and enhances the trapping effect. This synergism functions to tightly close the α-site and sends an allosteric signal that stabilizes the closed structure of the β-site. These studies also support a mechanism for the escape of indoline through the α-site that is limited by ASL dissociation.

The $\alpha_2\beta_2$ tryptophan synthase bienzyme complex catalyzes the final two steps in the biosynthesis of tryptophan (*1*−*5*). The α-subunit is a 29 kDa eight-fold αβ-barrel enzyme that is structurally homologous to triose phosphate isomerase. The β-subunit is a PLP-requiring 40 kDa enzyme made up of two domains with the catalytic site and PLP located on the interface between the two domains (*6*). By examining the three-dimensional structure of the bienzyme complex taken from *Salmonella typhimurium*, Hyde et al. (*6*) showed that the α- and β-sites of each αβ-dimeric unit are connected by a 25 Å tunnel. The α-subunit catalyzes an aldolytic-like cleavage of 3-indole-D-glycerol 3′-phosphate (IGP)[1] to indole and D-glyceraldehyde 3-phosphate (G3P) (eq 1; Scheme 1A). The cleaved indole then migrates, via diffusion through the tunnel, to the β-site where the β-subunit catalyzes a condensation reaction with the PLP-bound α-aminoacrylate form of L-Ser, E(A-A), to give L-tryptophan (L-Trp) (eq 2; Scheme 1A) (*7*−*11*). The combined α- and β-reactions are designated as the αβ-reaction (eq 3).

$$\text{IGP} \rightleftarrows \text{indole} + \text{G3P} \quad (1)$$

$$\text{L-Ser} + \text{indole} \rightleftarrows \text{L-Trp} \quad (2)$$

$$\text{IGP} + \text{L-Ser} \rightleftarrows \text{G3P} + \text{L-Trp} \quad (3)$$

The β-reaction occurs in two stages (Scheme 1A). In stage I, L-Ser reacts with the internal aldimine, E(Ain), and is converted to the quasi-stable E(A-A) species. In stage II (Scheme 1A), the indole released in the α-reaction is channeled via the tunnel to the β-site where it initiates C−C bond formation by nucleophilic attack on the β-C of E(A-A), producing a quinonoid intermediate, E(Q). The reaction then evolves through the L-Trp external aldimine and gem-diamine intermediates, finally regenerating E(Ain) with release of L-Trp.

† Supported by National Institutes of Health Grant RO1 GM055749.

* To whom correspondence should be addressed. Phone: (951) 852-4235. Fax: (951) 852-4434. E-mail: michael.dunn@ucr.edu.

‡ The Scripps Research Institute.

§ University of California.

[1] Abbreviations: ASL, α-site ligand; PLP, pyridoxal phosphate; L-Ser, L-serine; L-Trp, L-tryptophan; DIT, dihydroiso-L-tryptophan; IGP, 3-indole-D-glycerol 3′-phosphate; G3P, D-glyceraldehyde 3-phosphate; GP, α-glycerol phosphate; LDH, lactic dehydrogenase; NADH, reduced nicotinamide adenine dinucleotide; $\alpha_2\beta_2$, native tryptophan synthase from *S. typhimurium*; E(Ain), internal aldimine of PLP; E(A-A), enzyme-bound Schiff base of α-aminoacrylate; $E(Q_1)$, $E(Q_2)$, $E(Q_3)$, and $E(Q)_{indoline}$, quinonoid intermediates; $E(Aex_1)$, $E(Aex)_{DIT}$, and $E(Aex_2)$, external aldimine intermediates; TEA, triethanolamine buffer; BZI, benzimidazole; ANS, 8-anilino-1-naphthalenesulfonate; F9, *N*-(4-trifluoromethoxybenzenesulfonyl)-2-amino-1-ethyl phosphate.

10.1021/bi0516881 CCC: $30.25
Published on Web 12/02/2005

Scheme 1[a]

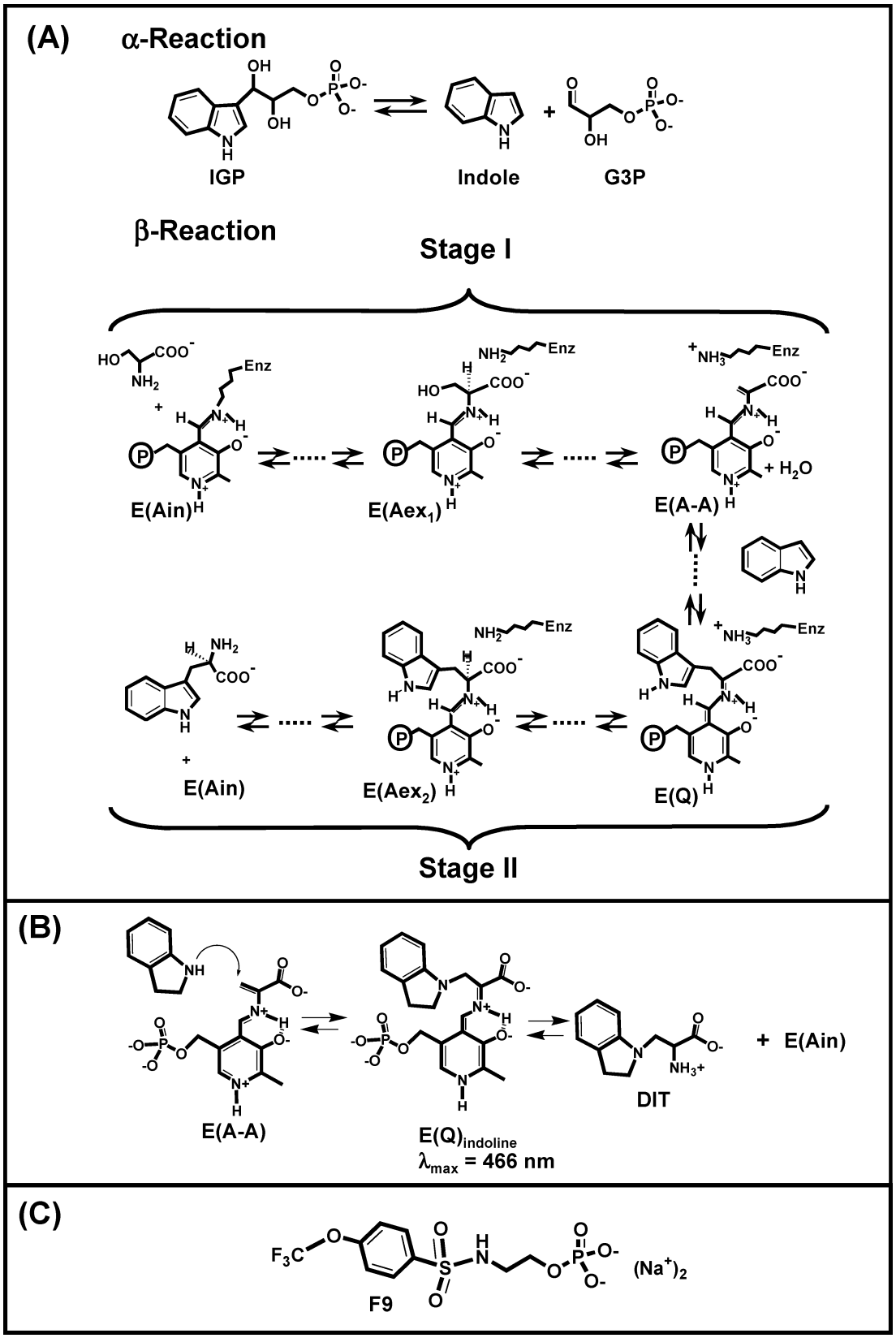

[a] (A) Physiological reactions catalyzed by tryptophan synthase. In the α-reaction, IGP is cleaved into indole and G3P. In the *β*-reaction, L-Ser forms E(A-A) in stage I. Indole reacts with E(A-A) to form L-Trp in stage II. (B) Reaction of indoline with the α-aminoacrylate intermediate, E(A-A), to give the indoline quinonoid intermediate, $E(Q)_{indoline}$, which then undergoes conversion to dihydroiso-L-tryptophan (DIT) and regeneration of the internal aldimine, E(Ain). (C) Structure of the IGP analogue, F9.

The α- and *β*-subunits of the tryptophan synthase enzyme system have a unique set of allosteric signals that regulate substrate channeling (*12*). These signals ensure that the substrates are processed in a highly synchronized order and that the intermediate indole is channeled from the α- to *β*-subunit without being released into solution. To prevent

the release of indole from the enzyme during the $\alpha\beta$-reaction, both of the subunits adopt closed conformations that trap indole within the confines of the α- and β-sites and the tunnel (*7*−*9*, *13*−*16*). This trapping ensures the efficient conversion of IGP and L-Ser into G3P and L-Trp (eq 3). In previous work, Harris and Dunn (*17*) introduced the tryptophan analogue dihydroiso-L-tryptophan (DIT) (*18*) as a probe for investigating the allosteric regulation of substrate channeling with particular emphasis on the trapping of the channeled intermediate.

Tryptophan synthase cleaves DIT (*17*, *18*), releasing the indole analogue indoline and forming E(A-A) (eq 4).

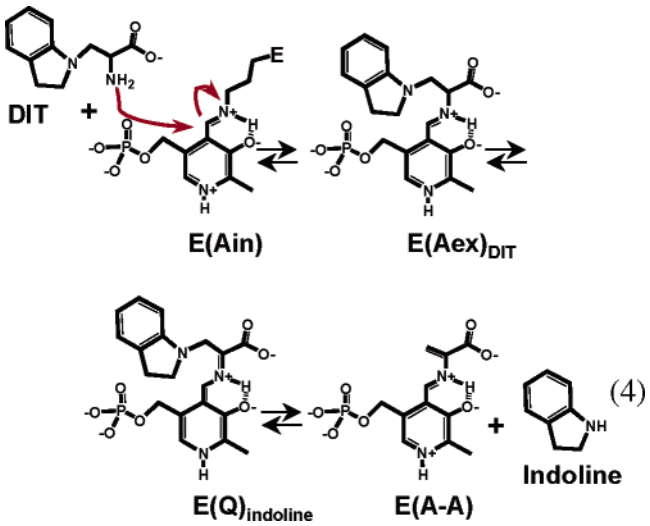

(4)

With the α-site ligand (ASL), GP, bound to the α-site, the $\alpha\beta$-dimeric units of the enzyme containing E(A-A) and $E(Q)_{indoline}$ are switched to closed conformations and the indoline formed in the interconversion of E(A-A) and $E(Q)_{indoline}$ (Scheme 1B; eq 4) is trapped within the closed enzyme (eq 5):

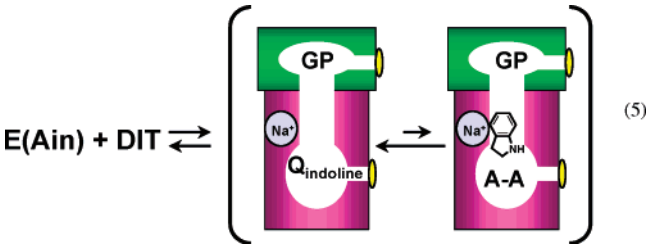

(5)

The mass action effect arising from the high local concentration of the trapped indoline causes the distribution of bound species to favor $E(Q)_{indoline}$. Because of the very large extinction coefficient of $E(Q)_{indoline}$, this species can be detected by its absorption spectrum with a λ_{max} of 466 nm (Scheme 1B). Ultimately, indoline leaks out into solution, and the 466 nm $E(Q)_{indoline}$ signal decays (*17*).

To examine the mechanism by which indoline escapes from closed $\alpha\beta$-dimeric units of the tetrameric enzyme during the DIT reaction, we consider three models for escape (Scheme 2). These models are designated as the α-site exit model, the closed−closed exit model, and the β-site exit model. In all three models, it is assumed that there is rapid interconversion among $E(Q)_{indoline}$, trapped indoline, and E(A-A) within closed $\alpha\beta$-subunit pairs.

α-Site Exit. In this hypothesis, the α-subunit simply switches to an open conformation, allowing the ASL to disengage, which allows the indoline to escape (Scheme 2). The binding dynamics of the ASL thus limits the rate of indoline escape.

Closed−Closed Exit. This hypothesis proposes that indoline escapes from the tunnel with both subunits of the $\alpha\beta$-pair in a closed conformation (Scheme 2). Two pathways for escape are of interest: (a) flexible, "breathing", motions which open a side wall pore in the tunnel of sufficient width for the escape of indoline and (b) subunits of an $\alpha\beta$-pair that transiently dissociate so that indoline can escape via the disconnected tunnel ends into solution.

β-Site Exit. In this model, either the E(A-A) at the closed β-site reacts back along the L-Ser reaction path to E(Ain) with release of L-Ser, or the E(A-A) undergoes a side reaction with water to form pyruvate and E(Ain). Either reaction would produce the open β-site conformation of E(Ain) through which indoline could escape (Scheme 2).

To investigate the mechanism of leakage, we undertake detailed equilibrium and kinetic investigations to compare the influence of ASL affinity on the transient formation and decay of $E(Q)_{indoline}$ during the reaction of DIT with E(Ain). The design and synthesis of a new ASL, *N*-(4-trifluoromethoxybenzenesulfonyl)-2-amino-1-ethyl phosphate (F9) (H. Ngo et al., manuscript in preparation) (*19*),[2] and the discovery of a strong synergism in the combined action of GP and benzimidazole (BZI) have made possible a more detailed study of the mechanism of indoline leakage in the DIT reaction that we report herein.

MATERIALS AND METHODS

Except as noted below, the materials and methods used were the same as those described in ref *17* and references therein.

Materials. The synthesis, purification, and characterization of *N*-(4-trifluoromethoxybenzenesulfonyl)-2-amino-1-ethyl phosphate (F9) will be described elsewhere (*19*).[2] All reactions were performed in 50 mM triethanolamine (TEA) buffer brought to a pH of 7.8 by the addition of HCl. All experiments with the enzyme were performed in the presence of 100 mM Na^+ to maintain the Na^+-activated form.

Kinetic Analysis of Rapid-Scanning and Single-Wavelength Absorbance Data. The analysis of relaxation kinetic data (*21*) was performed using Peakfit, version 4 (Jandel Scientific), and Sigma Plot 2001, version 7.0 (SPSS). The time courses were fit by the Marquardt−Levenberg algorithm to equations of the general form of eq 6:

$$A = A_0 \pm \sum A_n \exp\left(\frac{-t}{\tau_n}\right) \qquad (6)$$

where A and A_0 are the absorbance values at time t and at time infinity, respectively, and A_n is the amplitude of the nth relaxation, τ_n.

[2] Solution studies and X-ray crystallographic results have established that F9 binds with high affinity (Table 1), a stoichiometry of two per $\alpha_2\beta_2$ tetramer, and with high specificity to the α-sites of tryptophan synthase (*19*). The X-ray structure studies show a strong similarity between the structures of bound IGP (PDB entry 1QOQ) (*20*) and bound F9.

Scheme 2: Hypotheses for Indoline Leakage[a]

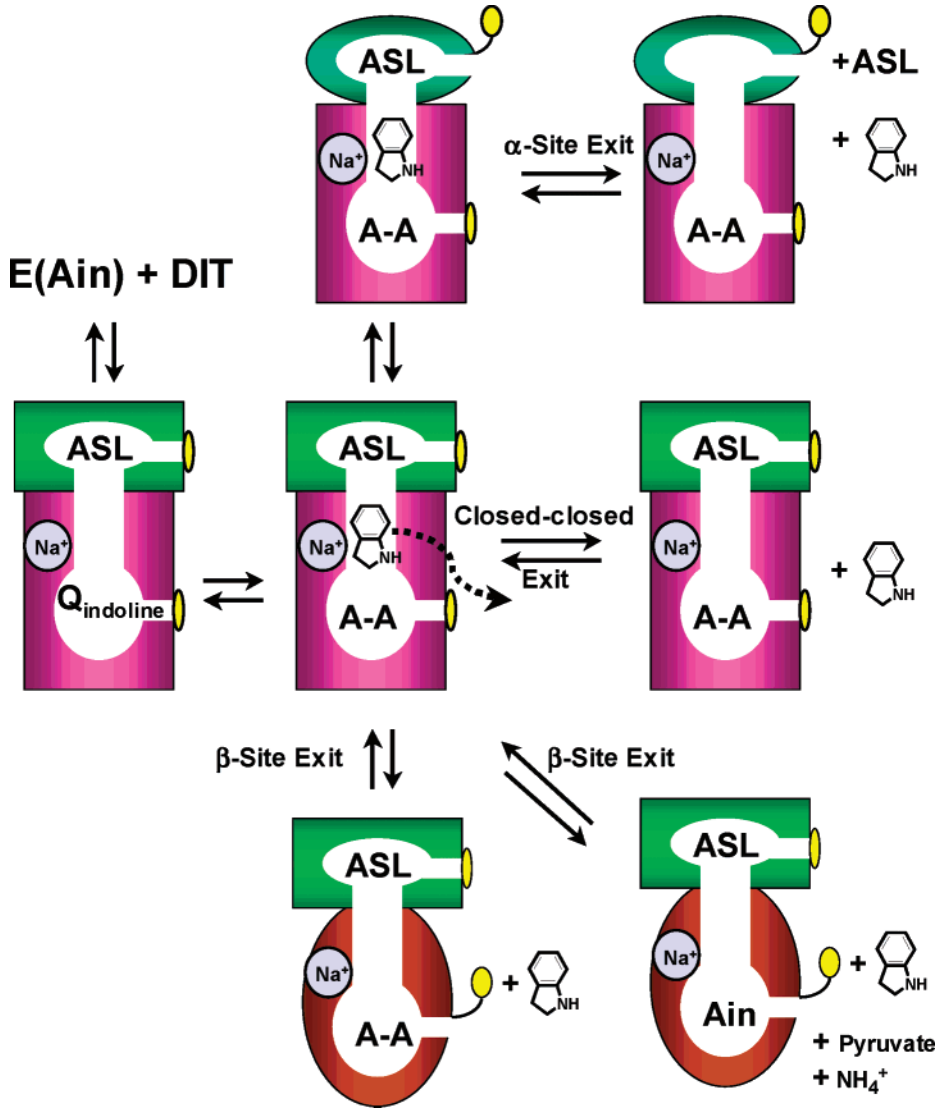

[a] Ovals and rectangles represent open and closed conformations, respectively.

Fluorescence Measurements. The fluorescence of ANS bound to tryptophan synthase was measured with a Spex Fluorolog II spectrofluorometer, equipped with a 150 W Xe source as previously described (*15*). The bound ANS was excited with 380 nm light, and emission spectra were recorded from 400 to 600 nm. A 1 mL solution containing 10 μM $\alpha_2\beta_2$, 100 mM Na^+, and 20 μM ANS in 50 mM TEA buffer was placed in a 3 mL cuvette. A Gilmont micrometer syringe pipet then was used to add a solution containing 10 μM $\alpha_2\beta_2$, 100 mM Na^+, 20 μM ANS, and 1.5 mM α-site ligand in 50 mM TEA in graduated amounts to increase the concentration of the ligand without changing the concentrations of the other components. The solution was added via a 0.5 mm diameter plastic tube inserted into the cuvette and stirred with a magnetic stir bar. The whole apparatus was covered in dark cloth to protect the solutions from light. Stopped-flow rapid-mixing fluorescence measurements to monitor the accumulation and decay of the $E(Aex_1)$ intermediate during the DIT reaction in the presence and absence of ASLs were performed as previously described (*7*, *14*, *15*).

Effects of ASLs on the Pyruvate Side Reaction. To test the influence of ASLs on the pyruvate side reaction, 40 mM L-Ser was combined with 10 μM $\alpha_2\beta_2$ to create the E(A-A) form of the enzyme. Pyruvate generated by the side reaction was detected by a coupled assay observing absorbance changes at 340 nm, wherein LDH converts NADH to NAD^+ as pyruvate is reduced to lactate (*22*).

RESULTS

Figure 1 shows time courses measuring the change in absorbance at 466 nm for the DIT reaction run both in the absence and in the presence of the ASLs, GP or F9.[2] In the presence of GP (trace b), there is a rapid increase in absorption as $E(Q)_{indoline}$ is formed, followed by a slower decrease in absorption as $E(Q)_{indoline}$ decays. In the absence of an ASL, there is no accumulation of $E(Q)_{indoline}$ (trace c). The transient accumulation of $E(Q)_{indoline}$ in the presence of GP was determined to be due to the trapping of the substrate intermediate indoline within the tunnel portion of the enzyme with the resulting accumulation of the $E(Q)_{indoline}$ intermediate (*17*) (eqs 5 and 10). Harris and Dunn (*17*) demonstrated that the increase in the magnitude of the signal is due to the accumulation of $E(Q)_{indoline}$ coupled to the mass action effect favoring $E(Q)_{indoline}$ over E(A-A) and indoline within closed $\alpha\beta$-dimeric units of the enzyme (viz., Scheme 1B and eq 5). Furthermore, the decay of the signal is due to the slow

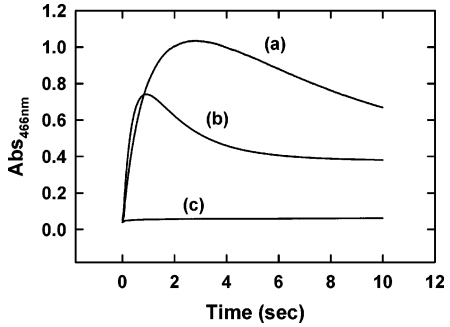

FIGURE 1: Comparison of the stopped-flow rapid-mixing time courses measured at 466 nm for the reaction of DIT with tryptophan synthase run in the presence of F9 (trace a) or GP (trace b) or in the absence of an ASL (trace c). Traces a and b show formation and decay of $E(Q)_{indoline}$, respectively, due to the transient trapping of indoline in the presence of F9 or GP. Trace c shows the time course in the absence of an ASL [notice the lack of formation and decay of $E(Q)_{indoline}$]. Concentrations: 20 μM $\alpha_2\beta_2$, 100 mM Na^+, 2 mM DIT, and, when present, 50 mM GP or 10 mM F9.

leakage of indoline into solution. In the absence of an ASL (trace c), there is no detectable (short-term) accumulation of $E(Q)_{indoline}$. It also was shown that the concentration of indoline released early in the reaction (e.g., the first 30 s) was too low to give detectable $E(Q)_{indoline}$ formation (*17*). Herein, we consider three possible paths for the leakage of indoline from the closed $\alpha\beta$-dimeric unit: α-site exit, β-site exit, and a closed−closed enzyme exit.

α-Site Exit Studies. The α-site exit hypothesis (Scheme 2) proposes that ASL dissociation involves the switch from a closed α-subunit conformation to an open conformation, allowing indoline to escape into solution. According to this mechanism, because the conversion of $E(Q)_{indoline}$ to E(A-A) with indoline trapped within the confines of the α- and β-sites and interconnecting tunnel is rapid, the rate of dissociation of the ASL limits the rate of the conformational transition to the open state, and therefore limits the rate of indoline escape. The dissociation constants for the different ASLs were determined by using the fluorescence of bound 8-anilino-1-naphthalenesulfonate (ANS) as a probe (*15*) (Table 1). Pan and Dunn (*15*) have shown that ANS bound to tryptophan synthase is highly fluorescent and that the binding of ASLs displaces ANS. The resulting quenching of ANS fluorescence gives a signal that can be used to determine apparent dissociation constants for ASL binding (*15*). The K_d values obtained for binding of GP and F9 to E(Ain) were 13.2 mM and 50.0 μM, respectively. The binding of these ligands to the E(A-A) form is strongly enhanced, giving values of 30.0 and 1.84 μM, respectively.

Figure 1 also compares the rapid-mixing stopped-flow time course for the reaction of DIT with E(Ain) preincubated with F9 (trace a) to the time course obtained in the presence of GP (trace b). The results show a transient formation ($1/\tau_1$) and decay ($1/\tau_2$) of $E(Q)_{indoline}$ when F9 is bound; however, there is a greater accumulation of $E(Q)_{indoline}$ because the indole leakage rate, $1/\tau_2$, is significantly slowed for the F9 system. The following $E(Q)_{indoline}$ relaxation rates were determined: $1/\tau_1 = 2.60\ s^{-1}$ and $1/\tau_2 = 0.50\ s^{-1}$ with GP and $1/\tau_1 = 1.20\ s^{-1}$ and $1/\tau_2 = 0.16\ s^{-1}$ with F9 (Table 1).

Closed−Closed Exit Studies. One mechanism for the closed−closed exit model of indoline leakage evokes a side wall exit in which a pore in the tunnel region opens, due to an enzyme breathing motion, and releases the trapped indoline. To investigate this possibility, the indole analogue benzimidazole (BZI) was used to investigate the dynamics of indoline transfer between the β-site and solution. BZI has been shown to be a reversible noncompetitive inhibitor of tryptophan synthase with binding interactions at the indole subsites of the α- and β-sites (*7*, *23*, *24*). When BZI enters the E(A-A) form of the enzyme, it binds relatively tightly to the indole subsite located at the β-site (*7*). This binding interaction strongly stabilizes the E(A-A). Due to the steric hindrance of BZI binding at the indole/indoline β-subsite, indoline is prevented from reacting with E(A-A) to form $E(Q)_{indoline}$. Conversely, when $E(Q)_{indoline}$ is mixed with BZI there is a rapid conversion of $E(Q)_{indoline}$ to the E(A-A)(BZI) complex and indoline (eq 7).

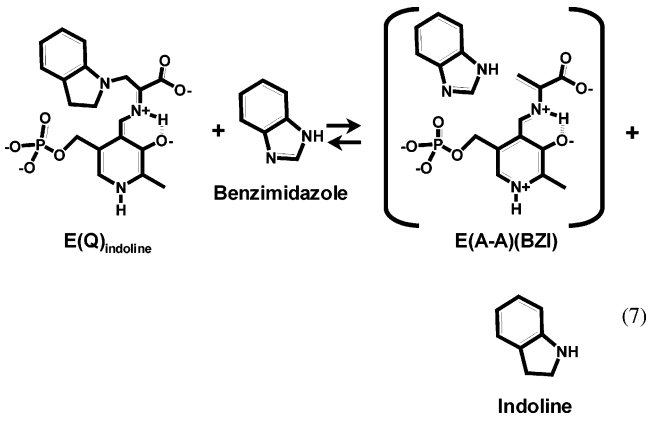

(7)

The time course for the displacement of indoline from $E(Q)_{indoline}$ has been shown to be strongly influenced by ASL binding (*7*, *13*). ASL binding stabilizes the α-site in the closed conformation, blocking access to the β-site via the α-site and the tunnel. Figure 2 shows time courses for the displacement of indoline from preformed $E(Q)_{indoline}$ by BZI, both with and without α-site ligands present. When $E(Q)_{indoline}$ is mixed with 2 mM BZI (trace c), there is a moderately rapid conversion ($1/\tau_1 = 13.01\ s^{-1}$) of $E(Q)_{indoline}$ to indoline and E(A-A)(BZI) (*7*) (eq 7). F9 binding slows the rate but not the yield of reaction by ~83-fold ($1/\tau_1 = 0.157\ s^{-1}$) (trace b), whereas the combination of GP and BZI slows the rate by ~900-fold ($1/\tau_1 = 0.0145\ s^{-1}$) (trace a). Consequently, the time course for displacement is sensitive to the structure of the ASL.

β-Site Exit Studies. According to the β-site exit hypothesis, for the indoline generated by cleavage of DIT to escape from the closed β-site of E(A-A), the β-subunit must be converted to the open conformation. Two mechanisms for conversion of E(A-A) to the open conformation of E(Ain) were considered. (a) The E(A-A) undergoes a side reaction with water, releasing pyruvate and NH_4^+ and forming E(Ain), or (b) the closed β-site of E(A-A) reacts back along the L-Ser reaction pathway, releasing L-Ser and forming E(Ain) (Scheme 2).

To test the influence of ASLs on the rate of conversion of L-Ser to pyruvate, the rate of this side reaction was detected by a coupled assay using LDH (*22*). The following rates of pyruvate production (k_{cat}) were obtained: $4.06 \times 10^{-3}\ s^{-1}$ no ASL, $2.13 \times 10^{-3}\ s^{-1}$ for GP, and $2.15 \times 10^{-3}\ s^{-1}$ for F9. Hence, both of these ASLs reduce the rate of pyruvate generation by a factor of only ~2.

Table 1: Comparison of Apparent Dissociation Constants for Binding of ASLs to E(Ain) and E(A-A), Relaxation Rate Constants for $E(Q)_{indoline}$ Formation and Decay in the DIT Reaction, and Steady-State Rates of Pyruvate Generation

			DIT reaction		
ASL	E(Ain) K_d[a] (μM)	E(A-A) K_d[a] (μM)	$E(Q)_{indoline}$ formation[b] $1/\tau_1$ (s^{-1})	$E(Q)_{indoline}$ decay[b] $1/\tau_2$ (s^{-1})	pyruvate production[c] (s^{-1})
none	–	–	–	–	5.7×10^{-3}
GP	13200 ± 970	30 ± 7	2.60 ± 0.006	0.50 ± 0.01	3.6×10^{-3}
F9	50 ± 5	1.84 ± 0.12	1.20 ± 0.06	0.16 ± 0.008	4.8×10^{-3}
GP and BZI[d,e]			0.143 ± 0.0005	0.016 ± 0.0002	1.4×10^{-3}
F9 and BZI[d,e]			0.538 ± 0.0005	0.103 ± 0.0015	1.4×10^{-3}

[a] Final concentrations of 10 μM $\alpha_2\beta_2$, 100 mM Na^+, 20 μM ANS, 40 mM L-Ser (when present), and varying ASL concentrations. [b] Final concentrations of 20 μM $\alpha_2\beta_2$, 100 mM Na^+, and either 50 mM GP or 10 mM F9 to which 2 mM DIT was added during mixing. [c] Final concentrations of 10 μM $\alpha_2\beta_2$, 100 mM Na^+, 40 mM L-Ser, 100 μM NADH, and a catalytic amount of LDH. [d] [BZI] = 2 mM. [e] Since BZI also binds at the β-site, meaningful measurements of K_d could not be measured.

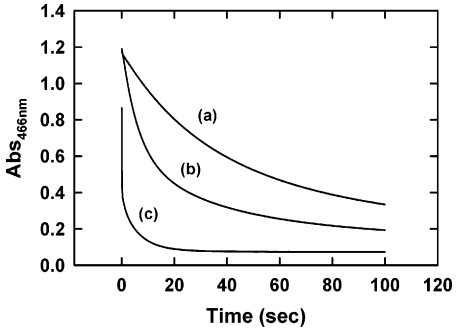

FIGURE 2: Displacement of indoline from preformed $E(Q)_{indoline}$ by BZI in the presence of (a) GP ($1/\tau_1 = 0.0145\ s^{-1}$) or (b) F9 ($1/\tau_1 = 0.157\ s^{-1}$) or (c) in the absence of an ASL ($1/\tau_1 = 13.01\ s^{-1}$). Concentrations: 10 μM $\alpha_2\beta_2$, 100 mM Na^+, 40 mM L-Ser, 50 mM indoline, 2 mM BZI, and, when present, 50 mM GP or 10 mM F9.

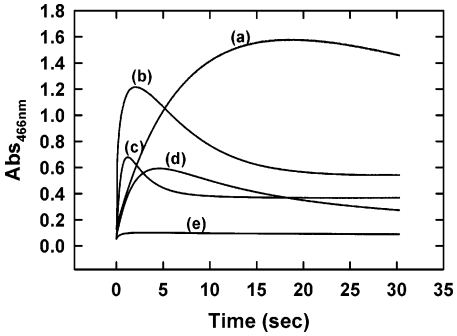

FIGURE 3: Effects of ASLs and BZI on the formation and decay of $E(Q)_{indoline}$ at 466 nm in the DIT reaction in the presence of GP or F9. $E(Q)_{indoline}$ trapping effect in the DIT reaction. The traces compare the effects of ASLs in the absence and presence of BZI on the formation and decay of $E(Q)_{indoline}$, ($1/\tau_1$ and $1/\tau_2$, respectively). Enzyme was preincubated with BZI and then mixed in the stopped-flow apparatus with GP and DIT. The values determined from analysis of the time courses are as follows: trace a, GP and BZI, $1/\tau_1 = 0.143\ s^{-1}$ and $1/\tau_2 = 0.016\ s^{-1}$; trace b, F9 alone, $1/\tau_1 = 1.20\ s^{-1}$ and $1/\tau_2 = 0.155\ s^{-1}$; trace c, GP alone, $1/\tau_1 = 2.47\ s^{-1}$ and $1/\tau_2 = 0.499\ s^{-1}$; trace d, F9 and BZI, $1/\tau_1 = 0.538\ s^{-1}$ and $1/\tau_2 = 0.103\ s^{-1}$; and trace e, BZI with no ASL (note curve is triphasic with two rising and one falling, all with very low amplitudes), $1/\tau_1 = 4.10\ s^{-1}$, $1/\tau_2 = 0.990\ s^{-1}$, and $1/\tau_3 = 0.066\ s^{-1}$.

Reaction of DIT back along the reaction pathway to release L-Ser and form E(Ain) could provide a mechanism for the escape of indoline. Stopped-flow rapid-mixing fluorescence measurements for monitoring the formation and decay of the $E(Aex_1)$ intermediate during the DIT reaction gave no indication of the accumulation of this species either in the absence or in the presence of ASLs (data not shown). Experiments also were performed comparing the reaction time courses for $E(Q)_{indoline}$ formation and decay where E(Ain) preincubated with GP in one syringe is reacted with DIT and varying amounts of L-Ser in the other syringe of the stopped-flow apparatus (data not shown). According to this mechanism, the presence of small amounts of L-Ser present with DIT should stabilize $E(Q)_{indoline}$ and thereby suppress the rate of indoline escape. Contrary to this prediction, no stabilization of $E(Q)_{indoline}$ was observed. When the reaction was performed with 0.10 or 0.50 mM L-Ser, a similar trapping of $E(Q)_{indoline}$ resulted, but with greatly reduced amplitudes. As the concentration of L-Ser was increased from 0 to 100 μM, and then to 500 μM, the decay rates ($1/\tau_2$) and amplitudes (absorbance at 466 nm) changed only slightly, from 0.50 s^{-1} (0.80 absorbance unit) to 0.68 s^{-1} (0.28 absorbance unit) and finally to 0.75 s^{-1} (0.16 absorbance unit), respectively. This result is consistent with a competition between L-Ser and DIT for reaction with E(Ain).

Synergistic Effects of BZI and GP on $E(Q)_{indoline}$ Trapping. Figure 3 shows the effects of BZI on the time courses for the DIT reaction conducted in the presence or absence of ASLs. When the reaction is run with the combination of GP and BZI (trace a), the $E(Q)_{indoline}$ formation and decay rates are both decreased in comparison to the values measured for GP alone (trace c). For the GP system, BZI binding slowed the $1/\tau_1$ rate from 2.47 to 0.143 s^{-1} (a 17-fold decrease), while $1/\tau_2$ changed from 0.50 to 0.016 s^{-1} (a 31-fold decrease, Table 1). Since $1/\tau_2$ is slowed more than $1/\tau_1$, there is a significant increase in the amplitude and duration of the absorbance at 466 nm, indicating a strong synergistic effect. Consequently, the combination of GP and BZI is more effective than GP alone in trapping $E(Q)_{indoline}$, and BZI alone (trace e) has no trapping effect. The time course in trace e reflects the absorbance change resulting from the redistribution of enzyme forms as DIT is converted to the E(A-A)-(BZI) complex and free indoline. In contrast to the synergistic behavior of the GP and BZI system, the combination of F9 and BZI gave much smaller rate changes: $1/\tau_1$ changed from 1.20 to 0.538 s^{-1} (a 2.2-fold decrease), while $1/\tau_2$ changed from 0.155 to 0.103 s^{-1} (a 1.5-fold decrease, Table 1). Thus, the combination of F9 and BZI (trace d) is less effective than F9 alone (trace b) and exhibits no synergism (Figure 3).

Influence of ASLs on DIT Turnover Rates. The effect of ASLs on the enzyme can also be measured by running the DIT reaction and concurrently examining the generation of

pyruvate with a coupled reaction (*22*). Table 1 shows a comparison of the k_{cat} values for pyruvate generation in the DIT reaction run in the presence of various ASLs with and without BZI. The three ASLs tested were shown to stabilize the E(A-A) form of the enzyme and thus reduce the rate of pyruvate generation by varying degrees when run without BZI. BZI alone was shown to stabilize the E(A-A) more than any of the ASLs alone do, a finding that is consistent with early observations (*7*). The greatest stabilization of E(A-A) is achieved when an ASL and BZI are both present, and these conditions give pyruvate generation rates that appear independent of ASL structure (Table 1).

DISCUSSION

In enteric bacteria, regulation of the *trp* operon ensures that the tryptophan synthase-mediated manufacture of L-Trp (and its precursor, IGP) is significant only when the operon is derepressed (*25*). Thus, the cell synthesizes IGP in response to a demand for L-Trp. In contrast to this situation, there is a sizable pre-existing pool of L-Ser in the cell. Consequently, under conditions in which the *trp* operon is activated and tryptophan synthase has been synthesized, the pre-existing pool of L-Ser should ensure that the predominating form of tryptophan synthase in vivo is the α-aminoacrylate intermediate, E(A-A). If this analysis is correct, then under physiological conditions, tryptophan synthase pre-exists as E(A-A), the species with the α-site activated for reaction with IGP in the first cycle of turnover (*8*, *26*, *27*). Woehl and Dunn (*16*) demonstrated that the steady-state rate of substrate turnover in the *β*-reaction (Scheme 1A) exhibits a primary kinetic isotope effect when [α-^{2}H]-L-Ser is substituted for isotopically normal L-Ser, indicating the conversion of E(Aex_1) to E(A-A) is rate-determining for turnover, whereas in the α*β*-reaction, L-Trp synthesis is accelerated and there is no isotope effect, indicating that the binding and/or reaction of IGP at the α-site alters the rate-determining step (*28*). The reaction of E(A-A) with IGP is orchestrated by a set of allosteric interactions that modulate the closing and opening of the α- and *β*-sites and the switching of the sites between high- and low-affinity/activity states that function to synchronize the activities of the two subunits and to prevent the escape of the channeled intermediate, indole (*5*, *7*−*12*, *29*). However, these allosteric interactions are incompletely understood. The work presented in this study further examines the allosteric effects arising from the binding of IGP by employing chemically stable IGP analogues and an L-Trp analogue to investigate the mechanism by which the α*β*-dimeric unit of tryptophan synthase is switched between open and closed states.

In the reaction of DIT with tryptophan synthase (eq 4), Harris and Dunn (*17*) demonstrated that the binding of the ASL, GP, to tryptophan synthase results in the transient trapping of the indoline quinonoid intermediate, $E(Q)_{indoline}$ (eq 5). The work presented herein shows that a new, higher-affinity ASL, F9, is more effective in trapping $E(Q)_{indoline}$. Furthermore, when the trapping reaction is performed with GP in the presence of BZI, the combination of GP and BZI is significantly more effective than either GP or F9 alone. These observations provide new insights with respect both to the mechanism of escape of indoline from the trap and to synergistic effects arising from ligand binding to the α-site.

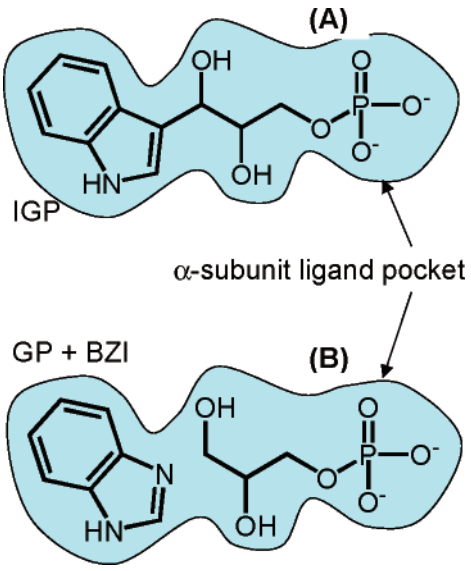

FIGURE 4: Cartoon comparing the proposed model for the binding of IGP (A) or the combination of GP and BZI (B) to the α-site. The combination of GP and BZI emulates the structure of IGP almost exactly, only replacing the covalent bond between the BZI ring and the glycerol C-3 atom with a van der Waals contact.

Synergistic Binding of BZI and GP to the α*-Site*. Figure 3 shows that in the absence of BZI, the indoline trapping effect is stronger and longer-lasting with F9 than with the weaker binding GP. In the examination of the BZI displacement of $E(Q)_{indoline}$ (see eq 7 and Figure 2), the question of why GP slows the displacement more than F9 arose, even though F9 binds more tightly to the α-site than does GP. Furthermore, in the DIT reaction, the combination of GP and BZI was found to be more effective than either GP alone or F9 alone in trapping $E(Q)_{indoline}$ (Table 1 and Figure 3), whereas F9 and BZI were less effective than F9 alone. BZI alone gave no trapping.

The most reasonable interpretation of these results is that BZI exerts a strong synergistic effect on the binding of GP at the α-site, but not on the binding of F9. As depicted in Figure 4, the simultaneous binding of GP and BZI could fill the α-site binding pocket, almost exactly mimicking the binding of the wild-type substrate, IGP. The synergism implied by this binding model then would account for the stronger effects arising from the combination of BZI and GP.

In the absence of an ASL, BZI also binds to the *β*-sites of both E(Ain) and E(A-A), but the affinity for E(A-A) is much greater (*7*). When BZI and GP are both present, the rate of $E(Q)_{indoline}$ formation in the DIT reaction is reduced (Table 1). For the DIT reaction run with GP in the absence of BZI, the rate of $E(Q)_{indoline}$ formation ($1/\tau_1$) equals 2.47 s^{-1}, whereas with BZI, the rate decreases and $1/\tau_1 = 0.143$ s^{-1}, a 17-fold reduction in rate. The corresponding rates with F9 in the absence and presence of BZI are 1.20 and 0.538 s^{-1}, respectively, an ∼2-fold reduction in rate. The rate of decay of the trapped $E(Q)_{indoline}$ also is greatly reduced by the combination of GP and BZI (31-fold), but almost unchanged by the combination of F9 and BZI (1.5-fold) (Table 1).

The large effects of BZI on both $1/\tau_1$ and $1/\tau_2$ in the presence of GP (Table 1) are curious in view of the relatively small effect of BZI in the presence of F9. The decrease in $1/\tau_1$ likely has two origins: binding of BZI to the *β*-site

weakly inhibits DIT binding and reaction, thus reducing the value of $1/\tau_1$, and/or the strong synergistic effect of GP and BZI may shift the distribution of conformations of the E(Ain) β-site toward the closed conformation, thus reducing the rate by restricting access of DIT to the β-site. Since BZI reduces the value of $1/\tau_1$ by only ~2-fold when the ASL is F9, it appears that inhibition of DIT binding by the binding of BZI to the β-site makes only a small contribution to the decrease in $1/\tau_1$. Since it is likely that DIT binding occurs via the open conformation, the stabilization of a closed conformation of the β-site of E(Ain) via the allosteric effects of ASL binding to the α-site likely is the major contribution to the reduction in $1/\tau_1$.

Escape of Indoline via Subunit Dissociation in an $\alpha\beta$-Closed Enzyme. The investigation of the mechanism by which trapped indoline escapes required the development of a plausible set of testable leakage models (see Scheme 2). Indoline generated by the DIT reaction could escape into solution via dissociation of the subunits through the newly opened end of the tunnel. If the trapped indoline escaped by this mechanism, then the rate of indoline leakage would be limited by the subunit dissociation rate. The rate of subunit dissociation has been determined in previous work for the *Escherichia coli* enzyme (*30*). That work demonstrated a two-step process (eq 8) where an isomerization of the β-subunit limited the rate of dissociation.

$$\alpha + \beta_2 \underset{k_{-1}}{\overset{k_1}{\rightleftharpoons}} \alpha\beta_2 \underset{k_{-2}}{\overset{k_2}{\rightleftharpoons}} \alpha\beta^*\beta \qquad (8)$$

The rate-limiting isomerization step, k_{-2}, was shown to have a rate of 9×10^{-4} s^{-1} in the absence of L-Ser or ASLs and a rate of $\sim 3 \times 10^{-5}$ s^{-1} in the presence of L-Ser (*30*). As can be seen from Table 1, the rates for the DIT-generated indoline leakage for either the GP or F9 complexes are 3 orders of magnitude greater than the rates for subunit dissociation, thus eliminating the possibility that indoline escapes via subunit dissociation as the major leakage pathway. The fact that the enzyme system has evolved to retain indole cleaved from IGP for a time period sufficient to allow reaction with the E(A-A) is consistent with the finding that the subunit dissociation rate is a significantly slower process. It is interesting that the pyruvate production rates (Table 1) are similar to the rate of subunit dissociation.

Escape of Indoline via a Side Wall Pore in an $\alpha\beta$-Closed Enzyme. This model assumes exit from a tunnel side wall pore (Scheme 2, a closed−closed exit model). It must be noted that any pathway that allows indoline to escape from the closed−closed form of the enzyme must also allow indoline (or its analogues) entry by the same path. Because of the rapid and reversible formation of $E(Q)_{indoline}$, BZI is able to rapidly displace the equilibrium for $E(Q)_{indoline}$ formation in favor of the E(A-A)(BZI) complex (*7*) (eq 7). When BZI is mixed with $E(Q)_{indoline}$, BZI enters the β-site via the α-site and the tunnel. However, the binding of an ASL greatly slows the entry of BZI into the β-site by blocking the α-site opening (*7*). As is seen in Figure 2, indoline is quickly displaced from $E(Q)_{indoline}$ in the absence of an ASL, and this displacement is slowed when an ASL is bound. If the entry path of BZI into the closed−closed conformation of the $(ASL)E(Q)_{indoline}$ complex occurred through some static side wall pore, then the entry rate should not depend on the structure of the bound ASL. Contradicting this prediction, the data presented in Figure 2 and Table 1 show that the leakage rate is strongly dependent on ASL structure.

When an ASL binds to the α-site, a conformation change is induced in the α-subunit (*6*, *7*, *10*, *11*, *16*, *19*, *20*, *31*−*36*). This conformational transition has been demonstrated by fluorescence energy transfer methods to significantly increase the rigidity of the β-subunit (*38*), and to alter the equilibrium distribution of intermediates in the β-reaction in favor of E(A-A) and $E(Q)_{indoline}$ (*8*, *27*, *31*). This induced rigidity likely would have the effect of restricting the breathing motions of the enzyme, and thus reduce the frequency of transient side wall passage formation. The binding of an ASL likely increases the enzyme rigidity and, therefore, could give a positive correlation between ASL binding affinity and the indoline leakage rates.

Escape of Indoline via the β-Site. Two types of mechanisms involving leakage of indoline from the β-site were considered (Scheme 2). One involves interconversion of closed and open conformations of E(A-A). If escape occurs via the conversion of the closed E(A-A) structure to an open E(A-A) structure, then the sensitivity of the rate of this conformational transition to the affinity of the ASL must be an allosteric effect.

The alternative mechanism involves the conversion of the closed conformation of E(A-A) to an intermediate on the reaction pathway with an open conformation, either $E(Aex_1)$ or E(Ain) (Scheme 2). Equation 9 shows three possible indoline escape routes (dashed lines), involving escape from $E(Aex_1)$, the E(Ain)(L-Ser) complex, or E(Ain).

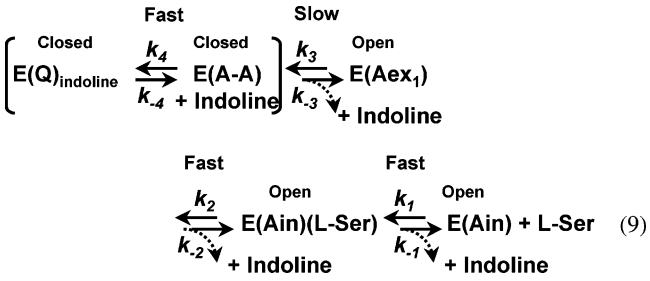

(9)

In eq 9, the E(Ain) and $E(Aex_1)$ species exist predominantly in the open conformation while the E(A-A) and $E(Q)_{indoline}$ species have the closed conformation (*15*). It is known that the k_1, k_{-1} and k_2, k_{-2} steps are fast (*27*, *37*) and that the k_4, k_{-4} step is also fast (*7*, *17*). When excess L-Ser is present, the equilibria in the absence of indoline favor conversion to a mixture dominated by $E(Aex_1)$ and E(A-A). When indoline is sequestered within the enzyme, then $E(Q)_{indoline}$ is favored (*17*). In the DIT reaction, no $E(Aex_1)$ fluorescence was detected, indicating there is no accumulation of this species. When the DIT reaction is run in the presence of low L-Ser concentrations (100 to 500 mM), the GP trapping of E(Q)indoline is not enhanced, suggesting that conversion to E(Ain) and L-Ser (eq 9) does not play a significant role in the escape of indoline.

When structures of the β-site with L-Ser bound are examined (for example, PDB entries 2TRS, 1KFJ, and 1BEU) (*16*, *32*, *36*), it can be seen that the reaction of L-Ser gives β-site structures where the passage between site and solution is partially blocked by the L-Ser moiety. The extent

to which the opening is blocked varies from structure to structure; however, in all of these structures, the opening appears to be too small to allow the passage of molecules the size of indole or indoline. These structures strongly suggest that indoline would not be able to escape from the β-site when sequestered within the E(Aex_1) or E(A-A) species. However, the opening from solution into the tunnel through the β-site appears to be sufficiently large in the E(Ain) structure to allow the passage of indole or indoline (see, for example, PDB entries 1BKS and 1KFK) (*36*). If the rate of conversion to E(Ain) limits the rate of indoline escape ($1/\tau_2$), then it is not obvious why the rate of this process would show such a strong dependence on the affinity of the ASL (Table 1).

Harris and Dunn (*17*) showed that in the DIT reaction, DIT ultimately is converted to pyruvate, NH_4^+, and E(Ain) via the side reaction of E(A-A) with water, thus potentially providing an alternative mechanism for the release of indoline. However, the 10−100-fold disparity in the rates of pyruvate formation and the values of $1/\tau_2$ (Table 1) indicates that the predominate leakage pathway does not occur via the pyruvate side reaction.

Escape of Indoline via the α*-Site Due to Dissociation of ASL from the* α*-Site*. Of the models that have been considered, the open α-site exit model provides the strongest correlation with the data. It was shown (*16*, *33*) that when an ASL binds to the α-site, loop αL6 folds over onto loop αL2, sequestering the ligand within the site. Visual examination of the external aldimine structures (PDB entries 1A50 and 1QOP) (*20*, *33*) with bound ASLs indicates there is too much steric hindrance at the α-site opening to allow the exit of a trapped indoline without a significant change in the α-subunit conformation. If indoline leakage were due to a rate-determining switching from a closed to an open conformation at the α-subunit followed by rapid dissociation of the ASL and indoline (Scheme 2, α-site exit model), then it is reasonable to expect that the rates of leakage should correlate with the apparent dissociation constants of the different ASLs. F9 binds to the α-site with significantly higher affinity than does GP (Table 1), and F9 is more effective in trapping $E(Q)_{indoline}$ (Figure 1). The increased yield of $E(Q)_{indoline}$ (Figure 1) results from a slower indoline leakage rate, $1/\tau_2$, suggesting that an increased binding affinity of the ASL decreases the rate of indoline escape. The correlation with affinity is further supported by the synergistic effects of BZI on the GP trapping of $E(Q)_{indoline}$ (Figure 3). The binding of BZI strongly enhances the affinity of the α-site for GP (Table 1), and the combination of GP with BZI gives a very slow indoline leakage rate (Table 1).

In summary, the discovery of the synergistic binding effects at the α-site between GP and BZI suggests that the more closely the ASL mimics the natural ligand, IGP, the stronger the trapping effect. The likely similarity of the ternary complex of GP and BZI to IGP is consistent with the previously proposed allosteric role of IGP in stabilizing the closed conformations of the E(A-A) and E(Q) species during the αβ-reaction (*12*, *14*, *27*, *28*).

We conclude that the most plausible mechanism for escape of indoline from the trapped $E(Q)_{indoline}$ intermediate involves leakage through the α-site triggered by dissociation of the α-site ligand. The evidence indicates that the alternative leakage mechanisms considered appear to be inconsistent with the observed rate and equilibrium data. However, the possibility of a side wall escape of indoline during enzyme breathing motions could not be discounted entirely. The high affinity of the new ASL, F9, renders this analogue much more effective than GP in trapping $E(Q)_{indoline}$, and the combination of GP and BZI was even more effective, thus strengthening the case for the α-site exit model.

REFERENCES

1. Yanofsky, C., and Crawford, I. P. (1972) Tryptophan synthase, in *The Enzymes* (Boyer, P. D., Ed.) Vol. 7, pp 1−31, Academic Press, New York.
2. Miles, E. W. (1979) Tryptophan synthase: Structure, function and subunit interaction, *Adv. Enzymol. Relat. Areas Mol. Biol. 49*, 127−186.
3. Miles, E. W. (1991) Structural basis for catalysis by tryptophan synthase, *Adv. Enzymol. Relat. Areas Mol. Biol. 64*, 93−172.
4. Miles, E. W. (1995) Proteins: structure, function and protein engineering, in *Subcellular Biochemistry* (Biswas, B. B., and Roy, S., Eds.) Vol. 24, pp 207−254, Plenum Press, New York.
5. Miles, E. W., Rhee, S., and Davies, D. R. (1999) The molecular basis of substrate channeling, *J. Biol. Chem. 274*, 12193−12196.
6. Hyde, C. C., Ahmed, S. A., Padlan, E. A., Miles, E. W., and Davies, D. R. (1988) Three-dimensional structure of the tryptophan synthase $\alpha_2\beta_2$ multienzyme complex from *Salmonella typhimurium*, *J. Biol. Chem. 263*, 17857−17871.
7. Dunn, M. F., Aguilar, V., Brzovic', P., Drewe, W. F., Houben, K. F., Leja, C. A., and Roy, M. (1990) The tryptophan synthase bienzyme complex transfers indole between the α- and β-sites via a 25−30 Å-long tunnel, *Biochemistry 29*, 8598−8607.
8. Brzovic, P. S., Sawa, Y., Miles, E. W., and Dunn, M. F. (1992) Evidence that mutations in a loop region of the α-subunit inhibit the transition from an open to a closed conformation in the tryptophan synthase bienzyme complex, *J. Biol. Chem. 267*, 13028−13038.
9. Brzovic, P. S., Hyde, C. C., Miles, E. W., and Dunn, M. F. (1993) Characterization of the functional role of a flexible loop in the α-subunit of tryptophan synthase from *S. typhimurium* by rapid-scanning stopped-flow spectroscopy and site-directed mutagenesis, *Biochemistry 32*, 10404−10413.
10. Lane, A. N., and Kirschner, K. (1991) Mechanism of the physiological reaction catalyzed by tryptophan synthase from *Escherichia coli*, *Biochemistry 30*, 479−484.
11. Anderson, K. S., Miles, E. W., and Johnson, K. A. (1991) Serine modulates substrate channeling in tryptophan synthase. A novel intersubunit triggering mechanism, *J. Biol. Chem. 266*, 8020−8033.
12. Pan, P., Woehl, E., and Dunn, M. F. (1997) Protein architecture, dynamics, and allostery in tryptophan synthase channeling, *Trends Biochem. Sci. 22*, 22−27.
13. Brzovic, P. S., Ngo, K., and Dunn, M. F. (1992) Allosteric interactions coordinate catalytic activity between successive metabolic enzymes in the tryptophan synthase bienzyme complex, *Biochemistry 31*, 3831−3839.
14. Weber-Ban, E., Hur, O., Bagwell, C., Banik, U., Yang, L.-H., Miles, E. E., and Dunn, M. F. (2001) Investigation of allosteric linkages in the regulation of tryptophan synthase: The roles of salt bridges and monovalent cations probed by site-directed mutation, optical spectroscopy, and kinetics, *Biochemistry 40*, 3497−3511.
15. Pan, P., and Dunn, M. F. (1996) β-Site covalent reactions trigger transitions between open and closed conformations of the tryptophan synthase bienzyme complex, *Biochemistry 35*, 5002−5013.
16. Rhee, S., Parris, K. D., Hyde, C. C., Ahmed, S. A., Miles, E. W., and Davies, D. R. (1997) Crystal structures of a mutant (βK87T) tryptophan synthase $\alpha_2\beta_2$ complex with ligands bound to the active sites of the α and β subunits reveal ligand-induced conformational changes, *Biochemistry 36*, 7664−7680.
17. Harris, R. M., and Dunn, M. F. (2002) Intermediate trapping via a conformational switch in the Na^+ activated tryptophan synthase bienzyme complex, *Biochemistry 41*, 9982−9990.
18. Roy, M., Keblawi, S., and Dunn, M. F. (1988) Stereoelectronic control of bond formation in *Escherichia coli* tryptophan synthase: Substrate specificity and enzymatic synthesis of the novel amino acid dihydroisotryptophan, *Biochemistry 27*, 6698−6704.

19. Ngo, H., Harris, R., Kimmich, N., Casino, P., Niks, D., Kulik, V., Schlichting, I., and Dunn, M. F. (2005) manuscript in preparation.
20. Weyand, M., and Schlichting, I. (1999) Crystal structure of wild-type tryptophan synthase complexed with the natural substrate indole-3-glycerol phosphate, *Biochemistry 38*, 16469−16480.
21. Bernasconi, C. (1976) *Relaxation Kinetics*, Academic Press, New York.
22. Crawford, I. P., and Ito, J. (1964) Serine deamination by the B protein of *Escherichia coli* tryptophan synthase, *Proc. Natl. Acad. Sci. U.S.A. 51*, 390−397.
23. Heilmann, H. D. (1978) On the mechanism of action of *Escherichia coli* tryptophan synthase. Steady-state investigations, *Biochim. Biophys. Acta 522*, 614−624.
24. Lane, A. N., and Kirschner, K. (1981) The mechanism of tryptophan binding to tryptophan synthase from *Escherichia coli*, *Eur. J. Biochem. 120*, 379−387.
25. Yanofsky, C., Konan, K. V., and Sarsero, J. P. (1996) Some novel transcription attenuation mechanisms used by bacteria, *Biochimie 78*, 1017−1024.
26. Leja, C. A., Woehl, E. U., and Dunn, M. F. (1995) Allosteric linkages between β-site covalent transformations and α-site activation and deactivation in the tryptophan synthase bienzyme complex, *Biochemistry 34*, 6552−6561.
27. Woehl, E., and Dunn, M. F. (1999) Mechanisms of monovalent cation action in enzyme catalysis: The first stage of the tryptophan synthase β-reaction, *Biochemistry 38*, 7118−7130.
28. Woehl, E., and Dunn, M. F. (1999) Mechanisms of monovalent cation action in enzyme catalysis: The tryptophan synthase α-, β- and $\alpha\beta$-reactions, *Biochemistry 38*, 7131−7141.
29. Bahar, I., and Jernigan, R. L. (1999) Cooperative fluctuations and subunit communication in tryptophan synthase, *Biochemistry 38*, 3478−3490.
30. Lane, A. N., Paul, C. H., and Kirschner, K. (1984) The mechanism of self-assembly of the multi-enzyme complex tryptophan synthase from *Escherichia coli*, *EMBO J. 3*, 279−287.
31. Houben, K. F., and Dunn, M. F. (1990) Allosteric effects acting over a distance of 20−25 Å in the *Escherichia coli* tryptophan synthase bienzyme complex increase ligand affinity and cause redistribution of covalent intermediates, *Biochemistry 29*, 2421−2429.
32. Rhee, S., Miles, E. W., and Davies, D. R. (1998) Cryo-crystallography of a true substrate, indole-3-glycerol phosphate, bound to a mutant (αD60N) tryptophan synthase $\alpha_2\beta_2$ complex reveals the correct orientation of active site αGlu49, *J. Biol. Chem. 273*, 8553−8555.
33. Schneider, T. R., Gerhardt, E., Lee, M., Liang, P.-H., Anderson, K. S., and Schlichting, I. (1998) Loop closure and intersubunit-communication in tryptophan synthase, *Biochemistry 37*, 5394−5406.
34. Sachpatzidis, A., Dealwis, C., Lubetsky, J. B., Liang, P. H., Anderson, K. S., and Lolis, E. (1999) Crystallographic studies of phosphonate-based α-reaction transition-state analogues complexed to tryptophan synthase, *Biochemistry 38*, 12665−12674.
35. Weyand, M., Schlichting, I., Marabotti, A., and Mozzarelli, A. (2002) Crystal structures of a new class of allosteric effectors complexed to tryptophan synthase, *J. Biol. Chem. 277*, 10647−10652.
36. Kulik, V., Weyand, M., Seidel, R., Niks, D., Arac, D., Dunn, M. F., and Schlickting, I. (2002) On the role of αThr 183 in the allosteric regulation and catalytic mechanism of tryptophan synthase. *J. Mol. Biol. 324*, 677−690.
37. Drewe, W. F., Jr., and Dunn, M. F. (1985) Detection and identification of intermediates in the reaction of L-serine with *Escherichia coli* tryptophan synthase via rapid-scanning ultraviolet−visible spectroscopy, *Biochemistry 24*, 3977−3987.
38. Strambini, G. B., Cioni, P., Peracchi, A., and Mozzarelli, A. (1992) Conformational changes and subunit communication in tryptophan synthase: effect of substrates and substrate analogs, *Biochemistry 31*, 7535−42.

BI0516881